New insights on coral mound development from groundtruthed high-resolution ROV-mounted multibeam imaging

Aaron Lim* [a)], Veerle A.I. Huvenne [b)], Agostina Vertino [c, d)], Silvia Spezzaferri [e)], and Andrew J. Wheeler [a, f)]

[a)] School of Biological, Earth and Environmental Sciences, University College Cork, Ireland

[b)] Marine Geoscience, National Oceanography Centre, University of Southampton Waterfront Campus, European Way, Southampton SO14 3ZH, UK

[c)] Ghent University, Department of Geology, Renard Centre of Marine Geology, Krijgslaan 281 S8, B-9000 Gent, Belgium

[d)] University of Milano-Bicocca, Department of Earth and Environmental Sciences, Piazza della Scienza 4, 20126 Milano, Italy

[e)] University of Fribourg, Department of Geosciences, Chemin du Musée, CH-1700 Fribourg, Switzerland

[f)] Irish Centre for Research in Applied Geosciences, University College Cork, Ireland

Abstract

Currents play a vital role in sustaining and developing deep water benthic habitats by mobilising food and nutrients to otherwise relatively barren parts of the seabed. Where sediment supply is significant, it can have a major influence on the development and

morphology of these habitats. This study examines a segment of the Belgica Mound Province, NE Atlantic to better constrain the processes affecting a small-sized cold water coral (CWC) mound habitat and conversely, the hydrodynamic influence of CWC mounds on their own morphological development and surroundings. Here, we utilise ROV-mounted multibeam, ROV-video data, and sediment samples to investigate current processes, mound morphology, density and development. Detailed mapping shows that the area may have the highest density of coral mounds recorded so far, with three distinct mound types defined based on size, morphology and the presence and degree of distinct scour features. A residual current of 36 - 40 cm s^{-1} is estimated while large scour features suggest low-frequency, high-magnitude events. These 3 mound types are i) smaller mounds with no scour; ii) mounds with scour in one to two distinct directions and; iii) larger mounds with mound encircling scour. The differing mound types likely had a staggered initiation where younger mounds preferentially developed near clusters of pre-existing mounds. Given the high density of these small CWC mounds, we support the hypothesis that over time, this clustering may eventually lead to these mounds coalescing into larger coral mound features.

Keywords: currents; sediments; bedforms; cold water coral mounds; habitat mapping

1. Introduction

Frame-building cold water corals (CWC) are sessile, filter-feeding organisms that can produce large three dimensional calcium carbonate skeletons and develop complex bioconstructions (Freiwald and Wilson, 1998; Zibrowius, 1980). Some species, such as *Lophelia pertusa* and

Madrepora oculata, occur worldwide and have the ability to exist in a range of settings, from large submarine canyons to contourite drifts and from the Indian Ocean to the Canadian Arctic (e.g. Davies and Guinotte, 2011; Edinger et al., 2011; Freiwald et al., 2004; Hargrave et al., 2004; Huvenne et al., 2011; Roberts et al., 2009; van Rooij et al., 2003). Frame-building CWC are typically found where a supply of food is concentrated and transported to the corals via enhanced currents (Davies et al., 2009). The three dimensional framework developed by the coral skeleton creates frictional drag, slowing the current causing the deposition of suspended particles (Wheeler et al., 2005). Continued deposition of sediments coupled with growth of CWC generates positive topographic features on the seabed called CWC mounds (De Mol et al., 2007; Victorero et al., 2016; Wheeler et al., 2008).

CWC mounds can range in height above the surrounding seabed from 10 m to 350 m (Henriet et al., 2014; Huvenne et al., 2005). Although development of CWC mounds tends to be episodic, dating of sediment cores from CWC mounds shows that mound growth can be as high as 120 cm ka^{-1} offshore Scotland (Douarin et al., 2013), 220 cm ka^{-1} offshore Ireland and between 600 and 1500 cm ka^{-1} offshore Norway (Wienberg and Titschack, 2015 and references therein). The current interglacial, the Holocene, has been particularly well-studied in terms of periods of CWC mound development (Frank et al., 2009; Wienberg and Titschack, 2015). During this period, the morphology of coral mounds is a result of the processes (e.g. currents) that have influenced them through their development (Huvenne et al., 2009a; Thierens et al., 2010; Wheeler et al., 2007; Wheeler et al., 2005). Early research showed that currents were among the main drivers for faunal distribution across coral mounds (Messing et al., 1990). More recently, direct measurements from current meters show that currents vary in velocity and regime across a coral mound and are likely to be the main control on coral distribution and therefore mound growth (Dorschel et al., 2007). The influence of currents on

mound development and morphology can also be seen across a number of small coral mounds where they elongate with prevailing current direction and become larger with increasing current velocity (Lim, 2017; Wheeler et al., 2008). Observations show that clusters of mounds develop an elongate pattern, corresponding to the direction of the highest currents speeds (Mienis et al., 2007). As such, CWCs are known to occur where currents are particularly high (Mohn et al., 2014). In support of this, long term measurements at coral mounds in the Rockall Trough, NE Atlantic show that low currents are one of the factors that limit coral growth on mound structures (Mienis et al., 2012).

More recently, Cyr et al. (2016) show that mound size has a direct influence on local hydrodynamics where larger mounds have a greater influence on hydrodynamics than smaller mounds. The same authors go on to show that CWC mounds create hydrodynamic turbulence, favourable for coral growth, and suggest that at a certain size flow can become blocked, detrimental to vertical growth of the mound.

Despite many studies carried out so far, the influence of environmental factors on mound density, morphology and size (and vice versa) is still poorly understood. This work focuses on the Moira Mounds region, a key study area characterised by densely-packed CWC mounds and well-defined, current-generated bedforms. It aims to better understand (1) the interactions between currents and CWC mound morphology and size and (2) the mechanisms that regulate coral mound development and coalescence.

1.1 Regional Setting

The Belgica Mound Province (BMP) is located on the eastern margin of the Porcupine Seabight: a large north-south embayment on the Irish continental margin, NE Atlantic (see Fig. 1) (Beyer et al., 2003; van Rooij et al., 2003). Part of the BMP exists within a Special Area of Conservation (SAC) designated under the EU Habitats Directive (https://www.npws.ie/). The main modern-day Porcupine Seabight water mass, which affects coral mound growth, is the Mediterranean Outflow Water (MOW) (De Mol et al., 2005; Rice et al., 1991; White et al., 2005) characterised by a salinity maximum between 600 m and 1100 m water depth. At this depth, temperatures are approximately 10°C with relatively high residual current speeds (White and Dorschel, 2010).

The BMP is known for its abundance of coral mounds(Wheeler et al., 2005). Large coral mounds occur in 2 distinct chains oriented parallel to the continental shelf (Fig. 1); the eastern chain is largely moribund (with a mainly dead coral cover; Foubert et al., 2005) while the western chain is mostly active with a profusion of live coral (De Mol et al., 2007; Dorschel et al., 2007; Eisele et al., 2008). These large coral mound morphologies range from conical to elongate, ridge-like forms and are typically 1 km across and 100 m tall (Beyer et al., 2003; Wheeler et al., 2005). Contourite drifts have accumulated between the giant (~100 m in height) carbonate mounds and buried their upslope flanks (van Rooij et al., 2003). Smaller CWC reefs, typically 30 m across and 10 m tall, are found throughout the BMP and are referred to as the "Moira Mounds" (Foubert et al., 2005; Kozachenko, 2005; Wheeler et al., 2005; Wheeler et al., 2011). These are divided into 4 zones (Fig. 1) based on their geographic distribution: upslope area, down-slope area, mid-slope area and northern area (see Wheeler et al., 2011). The Moira Mounds in the northern and upslope areas are dormant (Wheeler et al., 2011) while the Moira Mounds in the mid-slope area have been described as "sediment stressed", where they are being smothered by sediments (Foubert et al., 2011). A blind

channel, referred to as "Arwen Channel" (Fig. 1) (Murphy and Wheeler, 2017; Van Rooij, 2004), formerly connected to the shelf break, runs through the province and now contains the westernmost Moira Mounds studied here (referred from here on as downslope Moira Mounds).

Wheeler et al. (2011) hypothesise that the Moira Mounds may represent an early-stage "start-up" phase of the nearby, large Belgica coral mounds, noting that the "footprints" of clusters of Moira Mounds have a comparable size to the base of the giant cold-water coral mounds which, as such, may have formed through a coalescing of smaller coral mounds at early stages of their development (see also De Mol et al., 2005; Huvenne et al., 2005).

<INSERT FIGURE 1>

2 Materials and Methods

2.1 ROV-mounted High-Resolution Multibeam Echosounder

ROV-mounted multibeam echosounder (MBES) data were collected over the downslope Moira Mounds area during the QuERCi survey (2015) on board RV Celtic Explorer with the Holland 1 ROV (cruise number CE15009: Wheeler et al. (2015)). A high-resolution, dual-head Kongsberg EM2040 MBES was integrated with a sound velocity probe and mounted on the front-bottom of the ROV. Data were acquired at a frequency of 300 kHz while the ROV maintained a height of approx. 150 m above the seabed with a survey speed of approximately 2 knots. This achieved a swath width of approx. 400 m. Positioning and attitude were obtained using a Kongsberg HAINS inertial navigation system, ultra-short baseline (USBL) system (Sonardyne Ranger 2) and doppler velocity log (DVL). Data acquisition was carried out using

SIS software, where calibration values, sensor offsets, real-time sound velocity, navigation and attitude values were incorporated. Seven lines ranging from 850 m to 4.2 km long were collected over the downslope Moira Mound study site. It is worth noting that, although rare, the DVL mistriggered during data acquisition, affecting limited stretches of the raw navigation data. The MBES data were stored as *.all and *.wcd files and were processed using CARIS HIPS and SIPS v9.0.14 to apply tidal corrections and clean anomalous data spikes. The cleaned data were saved as a single *.xyz and gridded to a 0.5 m ArcView GRID.

The 0.5 m MBES grid was imported into ArcMap 10.4 and projected in UTM Zone 29N. Slope (degrees) and aspect were derived from the bathymetry using the Arc Toolbox Spatial Analyst tools.

The raw multibeam backscatter data were processed using the Geocoder algorithm in IVS Fledermaus. This algorithm removes all the gains used during acquisition and applies a series of radiometric and geometrical corrections to the original acoustic observations in order to obtain a correct value of backscatter strength (Fonseca et al., 2009). The processed file was saved as a geotiff. Throughout this manuscript, references to backscatter refer to relative backscatter strength.

2.2 Seabed Morphometric Analyses and Mound Density

To characterise the study area, distinguish between mound types and associated bedforms, morphometric analyses were carried out. Bathymetric grids, backscatter and slope of study area were plotted in ArcMap 10.4. Using a combination of these datasets, three main geomorphological features were identified: positive mound features, negative scour features and positive ridge-form features. Each individual feature was delineated manually within ArcMap and saved as a polygon *.shp files. The mound and scour polygons were used to

158 extract the pixel values from the bathymetric (depth), backscatter (backscatter strength) and
159 slope (slope angle) rasters. Individual mound height and scour depth were calculated by
160 subtracting the minimum bathymetric value from the maximum bathymetric value within
161 each of these mound and scour polygons using the Extract by Attributes tool. Similarly, mound
162 and scour polygon area, average backscatter, minimum slope, maximum slope and average
163 slope were calculated using the same tool and added to the polygon attribute table.

164 Mound volumes were calculated by:

165

166 $V = (A*H)/3$ (Eq. 1)

167

168 Where *V* is volume, *A* is area of base and *H* is height. This calculation assumes that the mound
169 is conical with an elliptic base. Calculated mound volumes were added to the attribute table
170 of the mound polygon.

171 The scour features were individually inspected, which resulted in a manual classification of
172 the mounds into three distinct types; a) mounds with one or two scour directions, b) mounds
173 with scour that encircles part or all of the mound and c) mounds without scour. This scour
174 classification was added to the mound polygon attribute table.

175 Using the kernel density tool in ArcMap Toolbox, a mound density distribution raster layer
176 was created. This calculated the density of the mound point features at each output raster
177 cell neighbourhood (460 m) and shows the number of mounds per square kilometre across
178 the study site. This was carried out for all the mounds within the area and separately for
179 mounds with one to two distinct scours and mounds with encircling scour.

2.3 ROV-mounted Video

In this study, ROV video data are used to groundtruth bathymetry and qualitatively assess mounds, scours and sediment types. ROV-video data were collected over downslope Moira Mounds during the VENTuRE survey (2011) (cruise number CE11009: Wheeler and shipboard party (2011)) and QuERCi survey (2015) (cruise number CE15009: Wheeler et al. (2015)) on board RV Celtic Explorer with the Holland 1 ROV (Fig. 2a). Video data were recorded using an array of HD and colour composite cameras including aft-facing, forward-facing and downward-facing cameras mounted on the HOLLAND 1 ROV. The ROV video survey speed was typically 0.3 - 0.4 kt. Positioning and navigation were achieved using a USBL (Sonardyne Ranger 2) and 1200 kHz RDI Workhouse DVL. The ROV altimeter recorded and logged the height of the ROV from the seabed. Parallel lasers set at 11 cm apart were used to scale video imagery. The ROV's forward-facing (navigation) sonar guided the ROV over the summit of each mound feature.

<INSERT FIGURE 2>

2.4 Sediment Sampling

Seven box cores from the downslope Moira Mounds are used in this study to estimate current velocities (Fig. 1b). They were collected using a NIOZ-type box corer during the Eurofleets Moira Mounds survey (2012) on board RV Belgica (Cruise Number 2012/16) in 980-1100 m of water, with pre-calibrated Global Acoustic Positioning System (GAPS) Ultra Short Base Line (USBL) navigation to an accuracy of 0.5% of the slant range. Sub-cores were taken from each retrieved box core, and were stored at 4°C.

For this study, only surface sediment samples from the box cores were used. The carbonate and organic component of the surface sediment was removed using 10% HCl and 10% H_20_2. Details of this carbonate and organic dissolution procedure can be found in Pirlet et al. (2011).

A 0.05 percent of sodium tetraphosphate solution was added to the remaining (lithic) component of the samples. The samples were shaken by hand and then sonicated for approximately 12 seconds to minimize flocculation of particles. Before particle-size analysis (PSA), the samples were mixed to ensure accurate representation of each sample. Laser granulometry was carried out at the Applied Geology Lab, University of Milano-Bicocca using a Malvern Mastersizer 2000. Each sample was added to the Malvern Mastersizer 2000 by means of liquid dispersion. Before measurement, ultrasonic waves were passed through the liquid to ensure full deflocculation of particles. Each sample was measured 5 times. The results were then averaged and stored as an excel file. Files were opened in GRADISTAT (see Blott and Pye, 2001) where mean grain sizes were automatically calculated using the Folk and Ward method (Folk and Ward, 1957).

2.5 Current Velocity Estimation

To understand the hydrodynamic regime around the Moira Mounds, erosional current thresholds were calculated after Soulsby (1997) (a detailed mathematical explanation can be found in Huvenne et al. (2009b)) to estimate current speeds where box-cores were retrieved. The mean grain size of each of these samples was used to estimate the critical current velocity 1 m above the seabed that would be required to allow grains to be transported in the water column. Grain sizes smaller than 10 µm were excluded from critical current velocity calculations as these are subject to flocculation (McCave et al., 1995).

Soulsby (1997) defines the formula to calculate the critical current velocity erosional threshold from particle size distributions as:

$\mathcal{U}_{100\,erosion} = \left(\frac{\mathcal{U}_{*cr}}{0.41}\right) \ln\left(\frac{z_{100}}{z_0}\right)$, where (Eq. 2)

z_{100} = level above seabed (1 m) (Eq. 2.1)

z_0 = roughness length, calculated = $\left(\frac{d}{12}\right)$ (Eq. 2.2)

d = grain diameter = mean of sample grain size curve (Eq. 2.2.1)

$\mathcal{U}_{cr}$ = critical shear velocity = $\mathcal{U}_{*cr} = \sqrt{\frac{\tau_{cr}}{\rho}}$, where (Eq. 2.3)

τ_{cr} = threshold bed shear stress (N/m^2) = (Eq. 2.3.1)

$g(\rho_s - \rho)d.\left(\frac{0.30}{1+1.2D_*} + 0.055[1 - \exp(-0.020D_*)]\right)$ (Eq. 2.3.1)

$\rho =$ water density = 1027.4 kg / m^3 (Eq. 2.3.2)

$\rho_s =$ grain density = 2650 kg / m^3 (quartz) (Eq. 2.3.3)

D_* = dimensionless grain size = $\left[\frac{g(\rho_s-\rho)}{\rho v^2}\right]^{\frac{1}{3}} d$ (Eq. 2.3.4)

v = kinematic viscosity of water

The use of this approach assumes that particle size reflects the benthic current regime. For our area of study where currents are strong, and sediment ripples are common, testifying to

241 extensive bedload sediment transport and sediment reworking, this assumption appears
242 valid.

243 In a second current estimation in support of the current strength calculations above, current
244 velocity estimation is applied via use of a bedform velocity matrix (see Stow et al., 2009). This
245 utilises mean grain size and bedform type to estimate current velocity, which can be read
246 directly from a graph therein.

247

248 # 3 Results

249 ## 3.1 Bathymetry, Slope and Acoustic Backscatter

250 An area of 4.6 km^2 was imaged with the multibeam echosounder. The bathymetric coverage
251 reveals a relatively flat seabed with megaripples punctuated by 106 distinct mound-like
252 features (the Moira Mounds) with associated scour pits and ridges throughout the downslope
253 Moira Mound study site. The bathymetric map (Figure 2a) shows the seabed gently sloping
254 from the deeper south to the shallower north (-1010 m to -942 m). The mounds are typically
255 4.9 m in height on average (a maximum height of 14.8 m) with a slightly elongated conical
256 morphology and relatively low backscatter. Distinct scour features occur around the mound
257 perimeters. These can occur as 1 or 2 smaller linear scours that extend from the mound
258 perimeter or encircle all or part of the mound perimeter. Scour features range from 66 m^2 to
259 9,093 m^2 (1,635 m^2 on average) reaching a scour depth of 3.6 m. Ridge-like features typically
260 occur to the south of the mounds (Fig. 2) and have an area from 70 m^2 to 6075 m^2 reaching a
261 height of up to 3.4 m. They typically occur in groups of 3 to 5, decreasing in size away from
262 the mounds, with an east-west orientated long-axis. Sinuous megaripples (sediment waves)
263 exist in the medium backscatter, off-mound area (Fig 2c). These have a wavelength of

approximately 10 m and a wave height of 20 cm to 75 cm, with a steepened, north-facing lee slope.

Figure 2b shows seabed slope angles relative to this data set with green characterising relatively flat seabed slopes whereas red and yellow characterises the steep seabed slopes. Features (mounds, scour, and ridges) are most easily identified on the maps of relative slope (Fig. 2b), acoustic backscatter (Fig 2c) or bathymetry (Fig 2a & 3). Acoustic backscatter is relatively constant throughout the area (Fig. 2c) with a slightly higher backscatter to the north, reflecting changing seabed properties (grainsize and roughness).

<INSERT FIGURE 3>

3.2 Geomorphological Features and Mound Density

The three geomorphological features identified and measured are positive mounds, negative scours and positive ridge-forms (Fig. 3). Mounds are typically clustered across the study site. Scour and ridge features occur only with mounds. Mounds can occur without scour (Fig. 3a), with poorly-developed scour (Fig. 3b and 3c) or with well-developed scour (Fig. 3d). Ridge-like features occur within the scour pits (Fig. 3d). As summarised in Fig. 4, mound backscatter ranges from -15 dB to -23 dB and scour backscatter ranges from -13 dB to -20 dB. Mound slope ranges from 7 to 32 degrees and scour slope ranges from 0.1 to 9 degrees. Mound volume ranges from 8 to 14,872 m^3 while scour depth ranges from 0.1 to 3.6 m.

<INSERT FIGURE 4>

The most obvious morphological distinction between mounds is presence/absence and degree of scour (poorly developed to well-developed). As such, three types of Moira Mounds are defined based on this morphological distinction (Fig. 5).

Type I mounds are defined based on their lack of scour (e.g. Fig. 3a). They are typically the smallest in volume (305 m^3 average, 247 m^3 median) (Fig. 5), predominantly occurring where other mounds are most dense (Fig. 6b). They are the least common mound type in the study area (22.6%). They have the lowest slope (average 17 degrees) and backscatter (average -19.1 dB) of the three mound types (Fig. 4). Ridge-like features rarely occur with these mounds (only 4 Type I mounds occur with ridges) (Fig. 5c).

Type II mounds are defined based on their poorly-developed scour that has formed along one sector of the mounds base (e.g. Fig. 3b and c). They are moderate in volume (1240 m^3 average, 748 m^3 median), more than twice the volume of most Type I mounds. They exist clustered throughout the study area (Fig. 6a) and are the most common mound type (50%). The scour that develops around these mounds covers an average area of 1,038 m^2 with an average depth of 0.5 m. These mounds have an average slope of 21° and an average backscatter of -18.5 dB; 45% of these mounds exist with ridges.

Type III mounds have well-developed scour, encircling all or most of the mound base (e.g. Fig. 3d). They are the largest in volume (2064 m^3 average, 1532 m^3 median), almost double the volume of Type II mounds. They exist throughout the study area but their highest density is to the immediate south of Type I and Type II mounds. They comprise 27.4% of the mounds in the study area. The scour that develops around these mounds covers an average area of 2,766 m^2 with an average depth of 0.9 m. These mounds have an average slope of 21° and an

306 average backscatter of -18.8 dB; 66% of these mounds typically exist with ridge-like features
307 within their scour pit (e.g. Fig 4D).

308 <INSERT FIGURE 5>

309 Mounds exist throughout the surveyed study site. However, the highest density of mounds,
310 >50 mounds/km^2, occurs in the largest cluster at the north of the study area (Fig. 6). The
311 lowest density of mounds (<10 mounds/km^2) typically exists outside these mound clustering
312 areas.

313 <INSERT FIGURE 6>

314 3.3 ROV-mounted Video

315 ROV-mounted video data (Fig. 2a) covers a total transect length of 8.7 km, crossing 17
316 mounds, scour and ridge-like features. Video observations confirm that the mounds and
317 ridge-like features are covered by coral while the scour pits are not. The mounds are
318 dominated by coral framework: *Lophelia pertusa* predominantly with *Madrepora oculata* in
319 places (Fig. 7a, b and c). The coral frameworks are typically 0.5 m to 1 m in height, protruding
320 from the mound surface. Live coral is more common near the mound summit while dead coral
321 frameworks occur mainly near the mound flanks.

322 The scour pits are sandy with some exposed dropstones and no coral present (Fig 7d and f).
323 Ridge-like features exist within some scour pits, adjacent to the mounds (Fig. 7d). Coral grows
324 at and near the summit of all observed ridge-like features, here called “coral ridges”, while
325 some coral rubble exists in troughs between ridges.

326 The off-mound areas are dominated by rippled sands with occasional gravel lags and
327 dropstones (Fig. 7e). The asymmetrical ripple crests are sinuous to lingoidal with a steepened
328 north-facing slope indicating a northerly-directed flow.

329 <INSERT FIGURE 7>

330 3.4 Current Velocity

331 The average erosional current velocity threshold for transporting the sand in the study area
332 is 36 cm s^{-1} (Table 1). Similarly, a current velocity of 35 - 40 cm s^{-1} was obtained by using the
333 bedform-velocity matrix with high-sinuousity megaripples and lingoidal megaripples and a
334 mean grain size of 235 µm.

335

336 <INSERT TABLE 1>

337 4. Discussion

338 4.1 Currents

339 The estimated sediment-derived current velocity of 36 cm s^{-1} and the bedform-derived
340 current velocity of 35 - 40 cm s^{-1} are coincident with each other as well as with direct current
341 velocity measurements close to our study area (34 cm s^{-1}) (Dorschel et al., 2007). The
342 bedforms observed here (megaripples/sandwaves) form over days to even weeks (Stow et
343 al., 2009) which, coupled with their persistence and common occurrence, suggests they
344 reflect a long-term, net effect of the current in shaping the seabed. As such, the steepened
345 lee slope of these megaripples indicates that the prevailing current is from south to north.
346 This flow is typical within the Porcupine Seabight (Pingree and LeCann, 1990; White, 2007).

However, the large scour pits, predominantly developed around the south-facing side of these mounds suggest a north-to-south flow direction. Given the prevailing current is south-to-north, the high energy required to form the scour pits and similarity of our independent current velocity estimates to nearby direct measurements, it is more likely that these scour pits are the result of high-magnitude, low-frequency current events. Furthermore, with the occurrence of dense water cascades reported previously from the Irish Margin (Hill et al., 1998) and the location of the study site within a south-north blind channel on the shelf break, we suggest that the low-frequency, high-magnitude events that form the scours may be dense water cascades flowing down the blind channel. Dense water cascades have been noted elsewhere reaching velocities up to 250 cm s^{-1} (Wilber et al., 1993). White et al. (2005) previously put forward the idea of dense water cascades in a CWC habitat in the NE Atlantic. Hill et al. (1998) also suggest that these dense water flows can be seasonal. Although no definitive explanation can be put forward for the mound encircling nature of some of the scour pits, this could be related to the pit becoming further shaped by the strong residual current or tidal influences in the area.

4.2 Mound Morphology

The downslope Moira Mounds show typically developed conical to elongate downstream morphology. The three different morphological types (I, II and III) we describe require further examination and may reflect evolutionary development stages.

Type I mounds are relatively small, with an average volume of approximately 300 m^3 and do not have scour or ridge-like features, whereas the much larger Type III mounds with an average volume of approximately 2,000 m^3 typically have well-developed scour and ridge-like

features. There is a developmental trend of scour and ridge-like features with increasing mound volume from Type I to Type II through to Type III mounds. Scour pits and ridge-like features are exclusively found in association with the mounds suggesting that a) the scour and ridges form under the influence of the mounds and b) that both features develop progressively with the increasing size of the mounds. A similar process has been observed and modelled around various other marine obstacles such as shipwrecks (Quinn, 2006; Smyth and Quinn, 2014) with the size of the obstacle influencing the hydrodynamic perturbation and, therefore the size of scour and drifts. As such, the mounds have a progressive influence on their local environment as they grow larger. These stages of development and influence are summarised in Figure 8.

<INSERT FIGURE 8>

Cold-water coral mounds with scoured bases are relatively common, for example in the Straits of Florida (Correa et al., 2012) and the Hedge Mounds, northwest Porcupine Bank, NE Atlantic (Dorschel et al., 2009). Of particular note are the Magellan Mounds which are an order of magnitude larger than the Moira Mounds but have moats that are enigmatically elongated and in some cases extended around the mounds (Huvenne et al., 2007). However, unlike other coral mounds with scour, coral ridges have developed in the scour pits of the Moira Mounds. This relationship has not been reported elsewhere. Since the ridges exist only within the main depressions of large, well-developed scour pits surrounding the mounds (typically Type III mounds), it appears that they develop after the scour formed and are potentially related to hydrodynamic effects as the mounds increase in size. While increased turbulence occurs within the main body of a scour pit around marine obstacles (Quinn and Smyth, 2017), Davies et al. (2009) show that turbulence induced by mound topography may account for

393 enhanced delivery of food particles suspended in deeper waters. The increased turbulence
394 means there can be concentration of suspended material which includes coral larvae can
395 settle and grow given the availability of suitable substrate. In addition, the concentration of
396 coarser materials (e.g. exposed dropstones) in the bottom of the scour may be this suitable
397 substrate for the coral to settle and grow upon. Moira Mounds further south of the study area
398 have been previously described as "substrate restricted", where the environmental
399 conditions and current speeds are favourable but there is a lack of hard substrate (Lim, 2017).

400 In terms of dimension, Type II and III mounds are typical of those described for the Moira
401 Mounds in the mid-slope, up-slope and northern areas (Wheeler et al., 2011). Both of these
402 mound types are large enough to be imaged in pre-existing map coverage (mapped using
403 deep-towed 30 kHz TOBI side scan sonar; see Huvenne et al. (2005)). However, the Type I
404 mounds are too small to be imaged by lower resolution pre-existing map coverage and do not
405 fit previous morphological descriptions of the other Moira-type Mounds (Huvenne et al.,
406 2005; Lim et al., 2017; Wheeler et al., 2005; Wheeler et al., 2011). Interestingly, Type I Moira
407 Mounds are similar in dimension (near circular, ~5 m in height) to the nearby Macnas Mounds,
408 which also occur on the eastern flank of the Porcupine Seabight but further up-slope at water
409 depths of 300 to 500 m (Wilson et al., 2007). Like the Type I Moira Mounds, the Macnas
410 Mounds occur within an eastern Porcupine Seabight channel, are notably small, have gentle
411 slopes and appear to be devoid of scour. Although speculative, their similarities and proximity
412 could suggest that the Macnas Mounds and the Type I Moira Mounds may have some
413 similarities in terms of their initiation and development.

414

415 4.3 Mound Density

The overall density of the downslope mounds in the study site is 22.9 mounds/km^{-2} (106 mounds in 4.64 km^2). The Moira Mounds and the Darwin Mounds in the northern Rockall Trough, UK waters were thought to be comparable in size and distribution (Huvenne et al., 2016; Huvenne et al., 2009a; Lim, 2017; Wheeler et al., 2011) although in our study area spatial density shows over an order of magnitude in difference. The NE Darwin Mounds have a spatial density of 1.28 mounds/km^{-2} (150 mounds per 117 km^2) and the NW Darwin mounds have a spatial density of 1.44 mounds/km^{-2} (75 mounds per 52 km^2) (http://jncc.defra.gov.uk). In comparison with other provinces of small mounds, the Atlantic-Moroccan margin has a low mound spatial density of 0.43 mounds/km^{-2} (781 mounds in 1,800 km^{-2}) (Vandorpe et al., 2017), the Santa Maria di Leuca (SML) mound province in the northern Ionian Sea has 9.7 mounds/km^{-2} (5,820 mounds in 600 km^{-2}) (Savini et al., 2014), the interfluves between the Dangeard and Explorer Canyons, NE Atlantic, which also has "minimounds" has 7.2 mounds/km^{-2} (400 mounds in approx. 55 km^{-2}) (Stewart et al., 2014) and coral mounds in the Straits of Florida on the Great Bahama Bank slope have 14 mounds/km^{-2}, which was subsequently described as a *major* mound region (Correa et al., 2012). As such, the downslope Moira Mounds may be described as a major and unique coral mound habitat given the high-spatial density of coral mounds of small sizes (~10 m in height), and even potentially the highest recorded density of coral mounds to date. It is worth noting that the coral mounds compared here vary in size and geographic range and therefore the total number of mounds occurring across the total geographic range of occurrence are compared.

4.4 The Influence of Mound Density on Mound Development

In terms of distribution, Type III mounds exist throughout the study area (Fig. 6). Assuming Type III mounds developed before Type II mounds, based on their size (approx. twice the volume of Type II mounds; Fig. 8), it appears that Type II mounds occur where Type III mounds are most densely distributed (Fig. 9). Similarly, assuming Type I mounds are younger than Type II and III, it appears that Type I mounds typically occur in the areas of highest mound density, as evident in the northern sector of the studied region (Fig. 6). This mound distribution can be compared with the distribution, at a smaller scale, of CWC isolated colonies and colonial aggregations in relation to dense and large CWC frameworks. Isolated colonies and coral aggregations (up to 2-3 m in extension) are typically observed in the basal part of the flanks of some Mediterranean and North Atlantic mounds (Rosso et al., 2010; Vertino et al., 2010; Wienberg et al., 2008) around larger and dense CWC frameworks. The initial settlement of coral larvae on suitable hard substrates generates new colonies that, growing on each other, tend to develop both vertically and laterally forming colonial aggregations. In turn, their neighbouring colonial aggregations can increase in size and, when in contact, merge to create dense and large coral frameworks. Similarly, younger type I mounds seem to occur at the periphery of larger ones supporting the idea of mound coalescence as a mechanism to propagate the development of giant mounds. The mound clusters studied herein have a comparable diameter and elongation as the surrounding "giant" Belgica coral mounds (Wheeler et al., 2011). Huvenne et al. (2009b) outline a model which can be applied for clusters of small mounds to grow into large mound bases where a limitation of sedimentation is required to not bury potential substrate, coral growth can keep up with sedimentation and, once they grow develop high enough, they escape continuous burial in the benthic boundary layer. As such, given their notably high spatial density,

462 continued development of Moira Mounds could lead to them coalescing into larger mounds
463 (Beyer et al., 2003; Huvenne et al., 2005; Wheeler et al., 2005).

464 It is thought that the distribution of the Moira Mounds is related to pre-existing topographic
465 features and suitable substrates such as current-aligned furrows and ridges as well as
466 dropstones (Foubert et al., 2011; Kozachenko, 2005; Wheeler et al., 2005). Presumably, larvae
467 of coral colonies have originally settled on these seafloor features generating isolated
468 colonies that, in favourable conditions, have evolved into loosely-packed coral aggregations
469 and then into dense frameworks. The lateral and vertical accretion of a CWC framework is
470 highly influenced by combined biological and sedimentological factors, such as the colony
471 growth rate, the generation of new corals through asexual and sexual reproduction (Brooke
472 and Järnegren, 2013; Dahl et al., 2012; Le Goff-Vitry, 2004; Waller and Tyler, 2005) and the
473 stabilising action of the sediment that accumulates at the coral base (Hebbeln et al., 2016).
474 Though recent studies on CWC larvae have highlighted the longevity and high dispersal
475 potential of Lophelia planulae (Strömberg and Larsson, 2017), it seems that there is a
476 significant retention of coral larvae within natal CWC sites (Le Goff-Vitry, 2004; Morrison et
477 al., 2011; Ross et al., 2017). The preferential coral larval settlement on suitable substrates
478 (such as tissue-barren skeletons of pre-existing colonies, coral rubble or other biogenic and
479 lithic surfaces) within natal reefs and/or in the surrounding areas may increase the potential
480 accretion of a single mound and favour the formation of densely packed mound clusters.

481 The dense mound distribution of the northern sector of the studied area could be linked to
482 favourable environmental conditions that lead coral larvae to preferentially settle in the
483 vicinity of the natal sites. However this observation must be corroborated by genetic studies
484 on coral colonies from the three different mound types. The preferential nucleation of coral

mounds in the surroundings of older ones, could also be favoured by the effects generated by mound clustering. As suggested by Vandorpe et al. (2017), mound clustering can intensify local bottom currents, thus improving food and sediment supply to mounds.

5. Conclusions

We conclude from estimations that a northerly-directed prevailing current of between 36 and 40 cm s^{-1} exists at the Moira Mounds, a current similar to direct current measurements obtained nearby. On the other hand, distinct scour features that have developed around the larger Moira Mounds suggest an opposing flow direction and may be the result of sporadic dense water cascades, common on continental slopes and previously observed on the Irish-Atlantic margin. Based on the presence/absence and degree of development of the scours, the downslope Moira Mounds can be classed into three types: Type I (small mounds with no scour); Type II (medium-sized mounds with poorly-developed scour) and; Type III (large mounds with well-developed scour and coral-ridges). Given their proximity and based on their size, it is likely that these mound types represent different ages where the smallest are the youngest. Ridge-like features occur within the large scour pits of the oldest (Type III) mounds. Unlike other mounds which form sediment tails (often called “comet marks”), this is the first case where such features are observed.

In addition, the downslope Moira Mounds represent the highest density of small-sized coral mounds recorded (22.9 per km^2). Previous studies have suggested that mound clustering has resulted in higher particle delivery to mounds (e.g. food and sediment) as a result of increased turbulence. Coincidently, the suggested younger Moira Mounds appear to preferentially develop within areas of highest mound density, supporting the idea that these mounds may

eventually coalesce, developing into the surrounding giant coral carbonate mounds in the Belgica Mound Province.

6. Acknowledgements

The authors thank Dr Mohit Tunwal and Nidia Alvarez (UCC) for mathematical proofing, Nicoletta Fusi (Uni. Milano-Bicocca) for guidance in laser granulometry, Dr Boris Dorschel for comments on an earlier version of this manuscript, Ms Zoë O' Hanlon and Ms Kim Harris for proof-reading. We are also very grateful to Gary Greene and one anonymous reviewer for their supportive and constructive comments. Authors would like to thank all cruise crew and scientific parties on RV Belgica (cruise number Belgica 12/18) and RV Celtic Explorer (cruise numbers CE15009 and CE11009) with Holland 1 ROV. RV Celtic Explorer cruises were grant aided by the Marine Institute under the Ship Time Programme of the National Development Plan, Ireland. The RV Belgica during the "Moira Mound cruise" was funded by the European Union Seventh Framework Programme (FP7/2007-2013), under the Eurofleets grant agreement n° 228344. This publication has emanated from research supported in part by a research grant from Science Foundation Ireland (SFI) under Grant Number 13/RC/2092 (co-funded under the European Regional Development Fund and by PIPCO RSG and its member companies) and 16/IA/4528 (co-funded by the Irish Marine Institute and the Geological Survey, Ireland) and by the Irish Research Council Graduate of Ireland Scholarship programme.

References

Beyer, A., Schenke, H.W., Klenke, M., Niederjasper, F., 2003. High resolution bathymetry of the eastern slope of the Porcupine Seabight. Marine Geology 198, 27-54.

Blott, S.J., Pye, K., 2001. GRADISTAT: a grain size distribution and statistics package for the analyses of unconsolidated sediments. Earth Surface Processes and Landforms 26, 1237-1248.

Brooke, S., Järnegren, J., 2013. Reproductive periodicity of the scleractinian coral Lophelia pertusa from the Trondheim Fjord, Norway. Marine Biology 160, 139-153.

Correa, T.B.S., Grasmueck, M., Eberli, G.P., Reed, J.K., Verwer, K., Purkis, S.A.M., 2012. Variability of cold-water coral mounds in a high sediment input and tidal current regime, Straits of Florida. Sedimentology 59, 1278-1304.

Cyr, F., van Haren, H., Mienis, F., Duineveld, G., Bourgault, D., 2016. On the influence of cold-water coral mound size on flow hydrodynamics, and vice versa. Geophysical Research Letters 43, 775-783.
Dahl, M.P., Pereyra, R.T., Lundälv, T., André, C., 2012. Fine-scale spatial genetic structure and clonal distribution of the cold-water coral Lophelia pertusa. Coral Reefs 31, 1135-1148.
Davies, A.J., Duineveld, G.C., Lavaleye, M.S., Bergman, M.J., van Haren, H., Roberts, J.M., 2009. Downwelling and deep-water bottom currents as food supply mechanisms to the cold-water coral Lophelia pertusa (Scleractinia) at the Mingulay Reef complex. Limnology and Oceanography 54, 620.
Davies, A.J., Guinotte, J.M., 2011. Global Habitat Suitability for Framework-Forming Cold-Water Corals. PLoS ONE 6, e18483.
De Mol, B., Henriet, J.-P., Canals, M., 2005. Development of coral banks in Porcupine Seabight: do they have Mediterranean ancestors?, in: Freiwald, A., Roberts, J.M. (Eds.), Cold-water Corals and Ecosystems. Springer, Berlin, Heidelberg, New York, pp. 515-533.
De Mol, B., Kozachenko, M., Wheeler, A.J., Alvares, H., Henriet, J.-P., Olu-Le Roy, K., 2007. Thérèse Mound: a case study of coral bank development in the Belgica Mound Province, Porcupine Seabight. International Journal of Earth Sciences 96, 103-120.
Dorschel, B., Hebbeln, D., Foubert, A.T.G., White, M., Wheeler, A.J., 2007. Hydrodynamics and cold-water coral facies distribution related to recent sedimentary processes at Galway Mound west of Ireland. Marine Geology 244, 184-195.
Dorschel, B., Wheeler, A.J., Huvenne, V.A.I., de Haas, H., 2009. Cold-water coral mounds in an erosive environmental setting: TOBI side-scan sonar data and ROV video footage from the northwest Porcupine Bank, NE Atlantic. Marine Geology 264, 218-229.
Douarin, M., Elliot, M., Noble, S.R., Sinclair, D., Henry, L.-A., Long, D., Moreton, S.G., Murray Roberts, J., 2013. Growth of north-east Atlantic cold-water coral reefs and mounds during the Holocene: A high resolution U-series and 14C chronology. Earth and Planetary Science Letters 375, 176-187.
Edinger, E.N., Sherwood, O.A., Piper, D.J.W., Wareham, V.E., Baker, K.D., Gilkinson, K.D., Scott, D.B., 2011. Geological features supporting deep-sea coral habitat in Atlantic Canada. Continental Shelf Research 31, S69-S84.
Eisele, M., Hebbeln, D., Wienberg, C., 2008. Growth history of a cold-water coral covered carbonate mound - Galway Mound, Porcupine Seabight, NE-Atlantic. Marine Geology 253, 160-169.
Folk, R.L., Ward, W.C., 1957. Brazos River bar: a study in the significance of grain size parameters. Journal of sedimentary research 27.
Fonseca, L., Brown, C., Calder, B., Mayer, L., Rzhanov, Y., 2009. Angular range analysis of acoustic themes from Stanton Banks Ireland: A link between visual interpretation and multibeam echosounder angular signatures. Applied Acoustics 70, 1298-1304.
Foubert, A.T.G., Beck, T., Wheeler, A.J., Opderbecke, J., Grehan, A., Klages, M., Thiede, J., Henriet, J.-P., Polarstern ARK-XIX/3a shipboard party, 2005. New view of the Belgica Mounds, Porcupine Seabight, NE Atlantic: preliminary results from the Polarstern ARK-XIX/3a ROV cruise, in: Freiwald, A., Roberts, J.M. (Eds.), Deep-water corals and Ecosystems, . Springer-Verlag, Berlin Heidelberg, pp. 403-415.
Foubert, A.T.G., Huvenne, V.A.I., Wheeler, A.J., Kozachenko, M., Opderbecke, J., Henriet, J.-P., 2011. The Moira Mounds, small cold-water coral mounds in the Porcupine Seabight, NE Atlantic: Part B - Evaluating the impact of sediment dynamics through high-resolution ROV-borne bathymetric mapping Marine Geology 282, 65-78.
Frank, N., Ricard, E., Lutringer-Paquet, A., van der Land, C., Colin, C., Blamart, D., Foubert, A.T.G., Van Rooij, D., Henriet, J.-P., de Haas, H., van Weering, T.C.E., 2009. The Holocene occurrence of cold water corals in the NE Atlantic: Implications for coral carbonate mound evolution. Marine Geology 266, 129-142.
Freiwald, A., Fosså, J.H., Grehan, A., Koslow, T., Roberts, J.M., 2004. Cold-water Coral Reefs, NEP-WCMC, Cambridge, UK, p. 88http://hdl.handle.net/20.500.11822/8727http://www.unep-wcmc.org/resources/publications/

UNEP_WCMC_bio_series/22.htm.

Freiwald, A., Wilson, J.B., 1998. Taphonomy of modern, deep, cold-temperate water coral reefs. Historical Biology 13, 37-52.
Hargrave, B.T., Kostylev, V.E., Hawkins, C.M., 2004. Benthic epifauna assemblages, biomass and respiration in The Gully region on the Scotian Shelf, NW Atlantic Ocean. Marine Ecology Progress Series 270, 55-70.
Hebbeln, D., Van Rooij, D., Wienberg, C., 2016. Good neighbours shaped by vigorous currents: Cold-water coral mounds and contourites in the North Atlantic. Marine Geology 378, 171-185.
Henriet, J.-P., Hamoumi, N., Da Silva, A.-C., Foubert, A., Lauridsen, B.W., Rüggeberg, A., Van Rooij, D., 2014. Carbonate mounds: from paradox to world heritage. Marine Geology 352, 89-110.
Hill, A.E., Souza, A.J., Jones, K., Simpson, J.H., Shapiro, G.I., McCandliss, R., Wilson, H., Leftley, J., 1998. The Malin cascade in winter 1996. Journal of Marine Research 56, 87-106.
Huvenne, V.A., Tyler, P.A., Masson, D.G., Fisher, E.H., Hauton, C., Huhnerbach, V., Le Bas, T.P., Wolff, G.A., 2011. A picture on the wall: innovative mapping reveals cold-water coral refuge in submarine canyon. PLoS ONE 6, e28755.
Huvenne, V.A.I., Bett, B.J., Masson, D.G., Le Bas, T.P., Wheeler, A.J., 2016. Effectiveness of a deep-sea cold-water coral Marine Protected Area, following eight years of fisheries closure. Biological Conservation 200, 60-69.
Huvenne, V.A.I., Beyer, A., de Haas, H., Dekindt, K., Henriet, J.-P., Kozachenko, M., Olu-Le Roy, K., Wheeler, A.J., participants, T.P.c., participants, C.c., 2005. The seabed appearance of different coral bank provinces in the Porcupine Seabight, NE Atlantic: results from sidescan sonar and ROV seabed mapping, in: Freiwald, A., Roberts, J.M. (Eds.), Cold-water Corals and Ecosystems. Springer-Verlag, Berlin Heidelberg, pp. 535-569.
Huvenne, V.A.I., Masson, D.G., Wheeler, A.J., 2009a. Sediment dynamics of a sandy contourite: the sedimentary context of the Darwin cold-water coral mounds, Northern Rockall Trough. International Journal of Earth Sciences 98, 865-884.
Huvenne, V.A.I., Shannon, P.M., Naeth, J., di Primio, R., Henriet, J.-P., Horsfield, B., de Haas, H., Wheeler, A.J., Olu-Le Roy, K., 2007. The Magellan mound province in the Porcupine Basin. International Journal of Earth Sciences 96, 85-101.
Huvenne, V.A.I., Van Rooij, D., De Mol, B., Thierens, M., O'Donnell, R., Foubert, A.T.G., 2009b. Sediment dynamics and palaeo-environmental context at key stages in the Challenger cold-water coral mound formation: Clues from sediment deposits at the mound base. Deep Sea Research Part I 56, 2263-2280.
Kozachenko, M., 2005. Present and Past Environments of the Belgica Mounds (deep-water coral carbonate mounds) Eastern Porcupine Seabight, North East Atlantic (unpublished PhD Thesis), Department of Geography and Geology. University College Cork, Cork, p. 221
Le Goff-Vitry, M.C., 2004. A deep-sea slant on the molecular phylogeny of the Scleractinia. Molecular Phylogenetics and Evolution 30, 167-177.
Lim, A., 2017. Spatio-temporal patterns and controls on cold-water coral reef development: the Moira Mounds, Porcupine Seabight, NE Atlantic, School of Biological, Earth and Environmental Sciences. University College Cork, Cork Open Research Archive, p. 221http://hdl.handle.net/10468/4031
Lim, A., Wheeler, A.J., Arnaubec, A., 2017. High-resolution facies zonation within a cold-water coral mound: The case of the Piddington Mound, Porcupine Seabight, NE Atlantic. Marine Geology 390, 120-130.
McCave, I.N., Manighetti, B., Robinson, S.G., 1995. Sortable silt and fine sediments size/composition slicing: Parameters for paleocurrent speed and palaeoceanography. Paleoceanography 10, 593-610.
Messing, C.G., Neumann, A.C., Lang, J.C., 1990. Biozonation of deep-water lithoherms and associated hardgrounds in the northeastern Straits of Florida. Palaios 5, 15-33.
Mienis, F., De Stigter, H.C., De Haas, H., Van der Land, C., Van Weering, T.C.E., 2012. Hydrodynamic conditions in a cold-water coral mound area on the Renard Ridge, southern Gulf of Cadiz. Journal of Marine Systems 96-97, 61-71.

637 Mienis, F., de Stigter, H.C., White, M., Duineveld, G., de Haas, H., van Weering, T.C.E., 2007.
638 Hydrodynamic controls on cold-water coral growth and carbonate-mound development at the SW and
639 SE Rockall Trough Margin, NE Atlantic Ocean. Deep-Sea Research I 54, 1655-1674.
640 Mohn, C., Rengstorf, A., White, M., Duineveld, G., Mienis, F., Soetaert, K., Grehan, A., 2014. Linking
641 benthic hydrodynamics and cold-water coral occurrences: A high-resolution model study at three
642 cold-water coral provinces in the NE Atlantic. Progress in Oceanography 122, 92-104.
643 Morrison, C.L., Ross, S.W., Nizinski, M.S., Brooke, S., Järnegren, J., Waller, R.G., Johnson, R.L., King,
644 T.L., 2011. Genetic discontinuity among regional populations of Lophelia pertusa in the North Atlantic
645 Ocean. Conservation Genetics 12, 713-729.
646 Murphy, P., Wheeler, A.J., 2017. A GIS-based application of drainage basin analysis and
647 geomorphometry in the submarine environment: The Gollum Canyon System, North-east Atlantic, in:
648 Bartlett, D., Celliers, L. (Eds.), Geoinformatics for Marine and Coastal Management. CRC Press, Taylor
649 & Francis Group, Boca Raton, USA.
650 Pingree, R.D., LeCann, B., 1990. Structure, strength and seasonality of the slope current in the Bay of
651 Biscay region. Journal of the Marine Biological Association of the United Kingdom 70, 857-885.
652 Pirlet, H., Colin, C., Thierens, M., Latruwe, K., Van Rooij, D., Foubert, A., Frank, N., Blamart, D.,
653 Huvenne, V.A., Swennen, R., 2011. The importance of the terrigenous fraction within a cold-water
654 coral mound: A case study. Marine Geology 282, 13-25.
655 Quinn, R., 2006. The role of scour in shipwreck site formation processes and the preservation of wreck-
656 associated scour signatures in the sedimentary record – evidence from seabed and sub-surface data.
657 Journal of Archaeological Science 33, 1419-1432.
658 Quinn, R., Smyth, T.A.G., 2017. Processes and patterns of flow, erosion, and deposition at shipwreck
659 sites: a computational fluid dynamic simulation. Archaeological and Anthropological Sciences.
660 Rice, A.L., Billett, D.S.M., Thurston, M.H., Lampitt, R.S., 1991. The Institute of Oceanographic Sciences
661 Biological Programme in the Porcupine Seabight: background and general introduction. Journal of the
662 Marine Biological Association of the United Kingdom 71, 281-310.
663 Roberts, J.M., Wheeler, A.J., Cairns, S., Freiwald, A., 2009. Cold-water corals: the biology and geology
664 of deep-sea coral habitats. Cambridge University Press.
665 Ross, R.E., Nimmo-Smith, W.A.M., Howell, K.L., 2017. Towards 'ecological coherence': Assessing larval
666 dispersal within a network of existing Marine Protected Areas. Deep Sea Research Part I:
667 Oceanographic Research Papers 126, 128-138.
668 Rosso, A., Vertino, A., Di Geronimo, I., Sanfilippo, R., Sciuto, F., Di Geronimo, R., Violanti, D., Corselli,
669 C., Taviani, M., Mastrototaro, F., Tursi, A., 2010. Hard- and soft-bottom thanatofacies from the Santa
670 Maria di Leuca deep-water coral province, Mediterranean. Deep-Sea Research II 57, 360-379.
671 Savini, A., Vertino, A., Marchese, F., Beuck, L., Freiwald, A., 2014. Mapping cold-water coral habitats
672 at different scales within the Northern Ionian Sea (Central Mediterranean): an assessment of coral
673 coverage and associated vulnerability. PLoS ONE 9, e87108.
674 Smyth, T.A.G., Quinn, R., 2014. The role of computational fluid dynamics in understanding shipwreck
675 site formation processes. Journal of Archaeological Science 45, 220-225.
676 Soulsby, R., 1997. Dynamics of marine sands, a manual for practical applications Thomas Telford.
677 London
678 Stewart, H.A., Davies, J.S., Guinan, J., Howell, K.L., 2014. The Dangeard and Explorer canyons, South
679 Western Approaches UK: Geology, sedimentology and newly discovered cold-water coral mini-
680 mounds. Deep Sea Research Part II: Topical Studies in Oceanography 104, 230-244.
681 Stow, D.A.V., Hernández-Molina, F.J., Llave, E., Sayago-Gil, M., Díaz del Río, V., Branson, A., 2009.
682 Bedform-velocity matrix: The estimation of bottom current velocity from bedform observations.
683 Geology 37, 327-330.
684 Strömberg, S.M., Larsson, A.I., 2017. Larval Behavior and Longevity in the Cold-Water Coral Lophelia
685 pertusa Indicate Potential for Long Distance Dispersal. Frontiers in Marine Science 4.
686 Thierens, M., Titschack, J., Dorschel, B., Huvenne, V.A.I., Wheeler, A.J., Stuut, J.-B.W., O'Donnell, R.,
687 2010. The 2.6 Ma depositional sequence from the Challenger cold-water coral carbonate mound (IODP

688 Exp. 307): sediment contributors and hydrodynamic palaeo-environments. Marine Geology 271, 260-
689 277.
690 Van Rooij, D., 2004. An integrated study of Quaternary sedimentary processes on the eastern slope of
691 the Porcupine Seabight, SW of Ireland. Ghent Universityhttp://dx.doi.org/1854/10815
692 van Rooij, D., De Mol, B., Huvenne, V.A.I., Ivanov, M.K., Henriet, J.-P., 2003. Seismic evidences of
693 current-controlled sedimentation in the Belgica mound province, upper Porcupine slope, southwest
694 of Ireland. Marine Geology 195, 31-53.
695 Vandorpe, T., Wienberg, C., Hebbeln, D., Van den Berghe, M., Gaide, S., Wintersteller, P., Van Rooij,
696 D., 2017. Multiple generations of buried cold-water coral mounds since the Early-Middle Pleistocene
697 Transition in the Atlantic Moroccan Coral Province, southern Gulf of Cádiz. Palaeogeography,
698 Palaeoclimatology, Palaeoecology.
699 Vertino, A., Savini, A., Rosso, A., Di Geronimo, I., Mastrototaro, F., Sanfilippo, R., Gay, G., Etiope, G.,
700 2010. Benthic habitat characterization and distribution from two representative sites of the deep-
701 water SML Coral Province (Mediterranean). Deep-Sea Research Part Ii-Topical Studies in
702 Oceanography 57, 380-396.
703 Victorero, L., Blamart, D., Pons-Branchu, E., Mavrogordato, M.N., Huvenne, V.A.I., 2016.
704 Reconstruction of the formation history of the Darwin Mounds, N Rockall Trough: How the dynamics
705 of a sandy contourite affected cold-water coral growth. Marine Geology 378, 186-195.
706 Waller, R.G., Tyler, P.A., 2005. The reproductive biology of two deep-water, reef-building
707 scleractinians from the NE Atlantic Ocean. Coral Reefs 24, 514.
708 Wheeler, A.J., Beyer, A., Freiwald, A., de Haas, H., Huvenne, V.A.I., Kozachenko, M., Olu-Le Roy, K.,
709 Opderbecke, J., 2007. Morphology and environment of cold-water coral carbonate mounds on the NW
710 European margin. International Journal of Earth Sciences 96, 37-56.
711 Wheeler, A.J., Capocci, R., Crippa, L., Connolly, N., Hogan, R., Lim, A., McCarthy, E., McGonigle, C., O'
712 Donnell, E., O' Sullivan, K., Power, K., Ryan, G., Vertino, A., Holland 1 ROV Technical Team, Officers and
713 Crew of the RV Celtic Explorer, 2015. Cruise Report: Quantifying Environmental Controls on Cold-
714 Water coral Reef Growth (QuERCi). University College Cork, Ireland
715 Wheeler, A.J., Kozachenko, M., Beyer, A., Foubert, A.T.G., Huvenne, V.A.I., Klages, M., Masson, D.G.,
716 Olu-Le Roy, K., Thiede, J., 2005. Sedimentary processes and carbonate mounds in the Belgica Mound
717 province, Porcupine Seabight, NE Atlantic, in: Freiwald, A., Roberts, J.M. (Eds.), Cold-water Corals and
718 Ecosystems. Springer-Verlag, Berlin Heidelberg, pp. 533-564.
719 Wheeler, A.J., Kozachenko, M., Henry, L.A., Foubert, A., de Haas, H., Huvenne, V.A.I., Masson, D.G.,
720 Olu, K., 2011. The Moira Mounds, small cold-water coral banks in the Porcupine Seabight, NE Atlantic:
721 Part A—an early stage growth phase for future coral carbonate mounds? Marine Geology 282, 53-64.
722 Wheeler, A.J., Kozachenko, M., Masson, D.G., Huvenne, V.A.I., 2008. Influence of benthic sediment
723 transport on cold-water coral bank morphology and growth: the example of the Darwin Mounds,
724 north-east Atlantic. Sedimentology 55, 1875-1887.
725 Wheeler, A.J., shipboard party, 2011. Vents & Reefs deep-sea ecosystem study of the 45˚ North MAR
726 hydrothermal vent field and the cold-water coral Moira Mounds, Porcupine Seabight, Cruise report,
727 p. 160
728 White, M., 2007. Benthic dynamics at the carbonate mound regions of the Porcupine Sea Bight
729 continental margin. International Journal of Earth Sciences 96, 1-9.
730 White, M., Dorschel, B., 2010. The importance of the permanent thermocline to the cold water coral
731 carbonate mound distribution in the NE Atlantic. Earth and Planetary Science Letters 296, 395-402.
732 White, M., Mohn, C., de Stigter, H.C., Mottram, G., 2005. Deep-water coral development as a function
733 of hydrodynamics and surface productivity around the submarine banks of the Rockall Trough, NE
734 Atlantic, in: Freiwald, A., Roberts, J.M. (Eds.), Cold-water Corals and Ecosystems. Springer, Berlin,
735 Heidelberg, New York, pp. 503-514.
736 Wienberg, C., Beuck, L., Heidkamp, S., Hebbeln, D., Freiwald, A., Pfannkuche, O., Monteys, F.X., 2008.
737 Franken Mound: facies and biocoenoses on a newly-discovered “carbonate mound” on the western
738 Rockall Bank, NE Atlantic. Facies 54, 1-24.

739 Wienberg, C., Titschack, J., 2015. Framework-Forming Scleractinian Cold-Water Corals Through Space
740 and Time: A Late Quaternary North Atlantic Perspective, in: Rossi, S., Bramanti, L., Gori, A., Orejas Saco
741 del Valle, C. (Eds.), Marine Animal Forests: The Ecology of Benthic Biodiversity Hotspots. Springer
742 International Publishing, Cham, pp. 1-34.
743 Wilber, R.J., Whitehead, J., Halley, R.B., Milliman, J.D., Wilson, P.A., Roberts, H.H., 1993. Carbonate-
744 periplatforrn sedimentation by density flows: A mechanism for rapid off-bank and vertical transport
745 of shallow-water fines: Comment and Reply. Geology 21, 667-669.
746 Wilson, M.F.J., O'Connell, B., Brown, C., Guinan, J.C., Grehan, A.J., 2007. Multiscale Terrain Analysis of
747 Multibeam Bathymetry Data for Habitat Mapping on the Continental Slope. Marine Geodesy 30, 3-35.
748 Zibrowius, H., 1980. Les Scléractiniaires de la Méditerranée et de l'Atlantique nord-oriental. Mémoires
749 de l'Institut océanographique, Monaco.

750

751 Figures

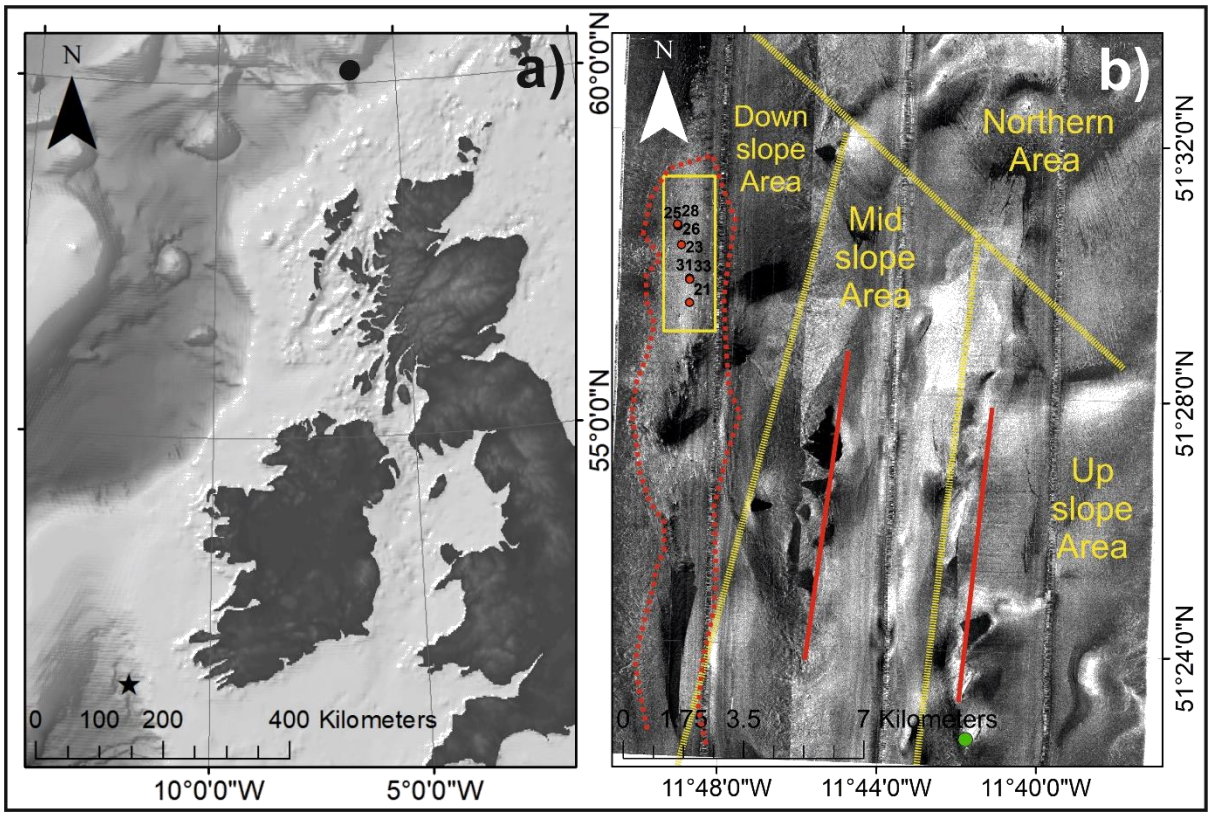

752

753 *Figure 1a) Locations of the Moira Mounds (star) and of Darwin Mounds (dot); 1b) TOBI 30 kHz*
754 *sidescan sonar map (after Huvenne et al., 2005) of the Moira Mounds area showing the*
755 *Challenger Mound (green dot), chains of giant coral carbonate mounds (red lines), margins of*
756 *blind channel (red dashed line), the 4 Moira Mound areas after Wheeler et al. (2011) (yellow*

dashed lines), the study site (solid yellow box) and locations of box cores used for this study (red dots).

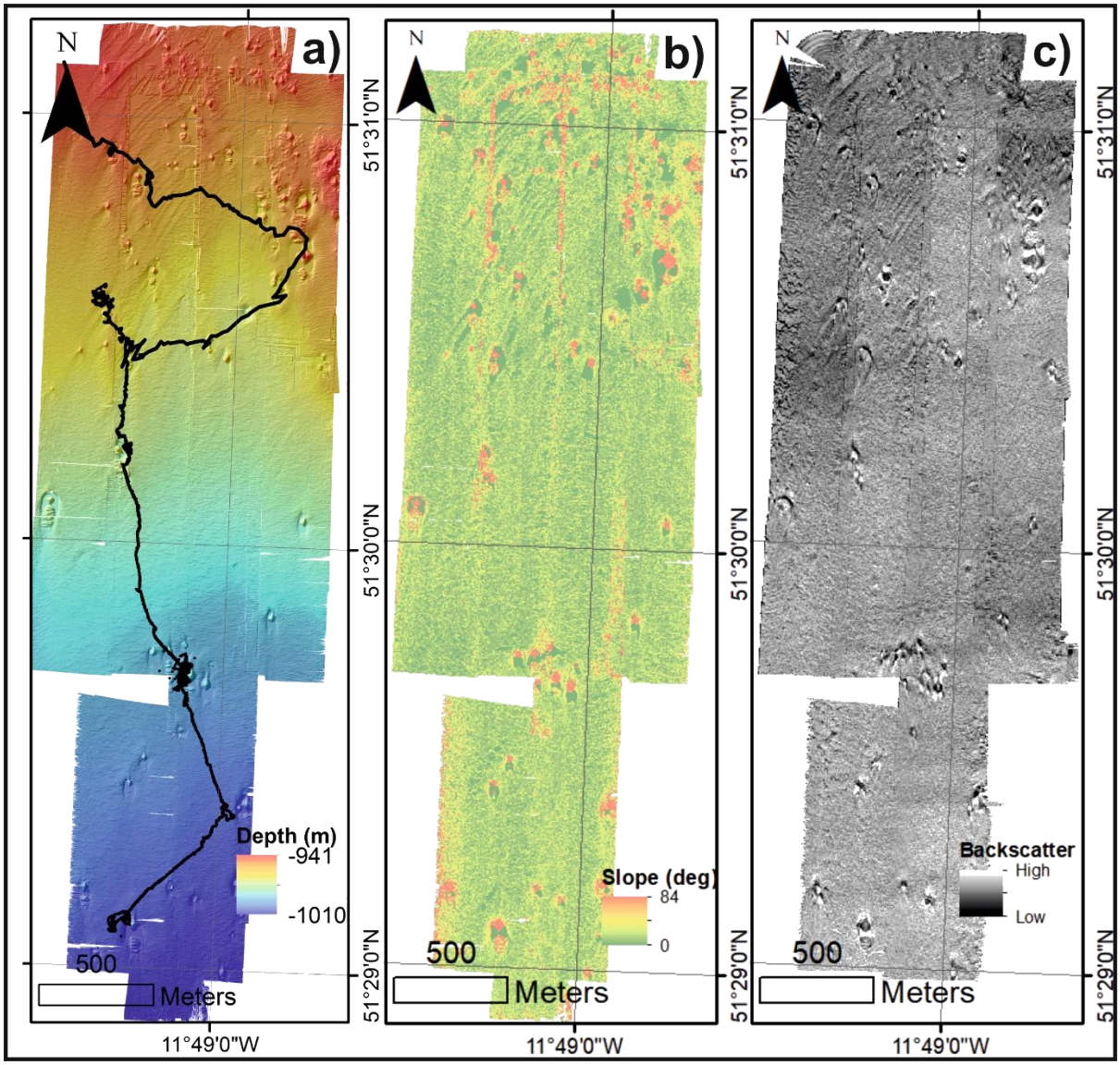

Figure. 2a) Multibeam echosounder bathymetric coverage with the ROV video groundtruthing line shown in black; 2b) seabed slope within the study area (degrees); 2c) multibeam echosounder backscatter (high backscatter in lighter tones, lower in darker tones)

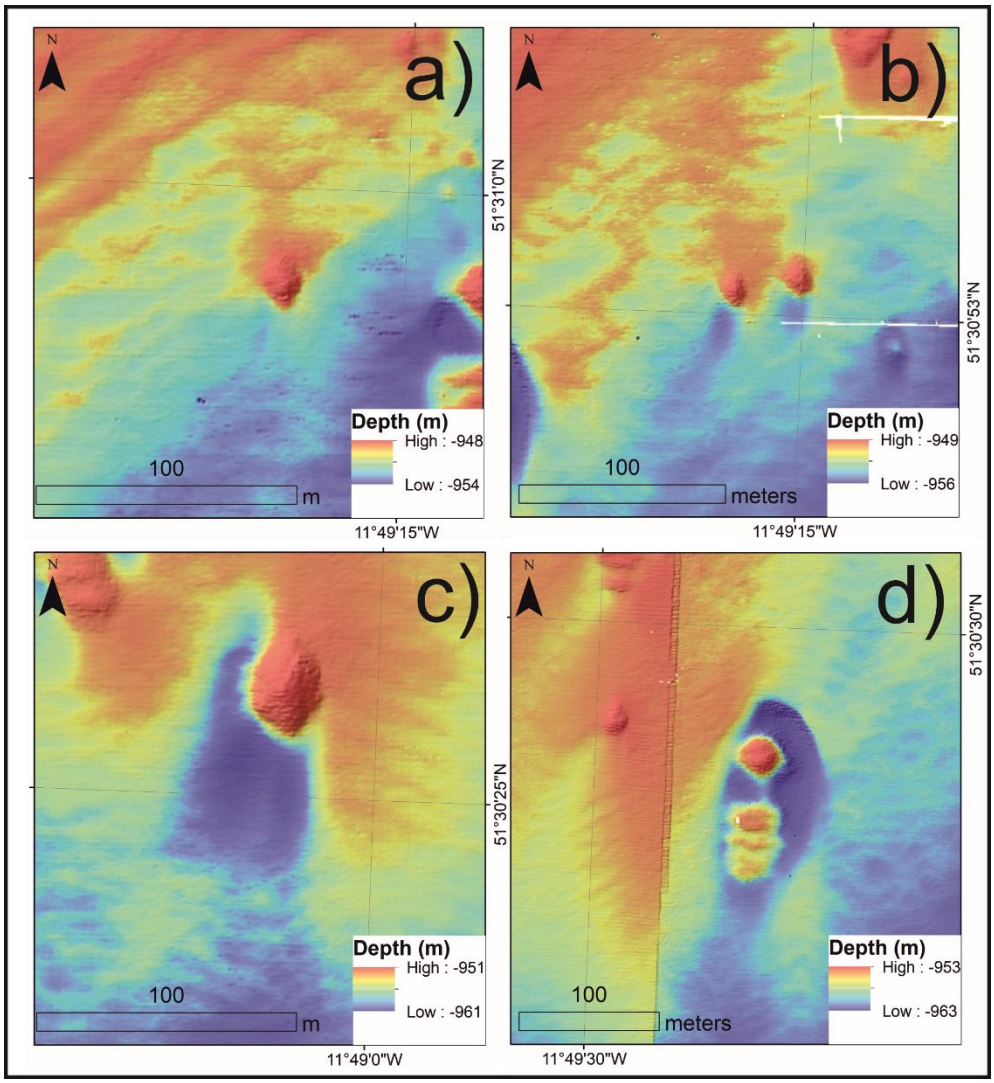

Figure 3 a) Bathymetric data showing a small Moira Mound approx. 3 m in height with no scouring, surrounded by a megarippled seabed; b) bathymetric data showing 2 small Moira Mounds with scour developing at 1 sector of the mound perimeter, surrounded by a megarippled seabed; c) bathymetric data showing a moderately-sized Moira Mound where the mound base has been scoured; d) bathymetric data showing a large Moira Mound with well-developed scour encircling the mound base with ridge-like features formed within the scour pit.

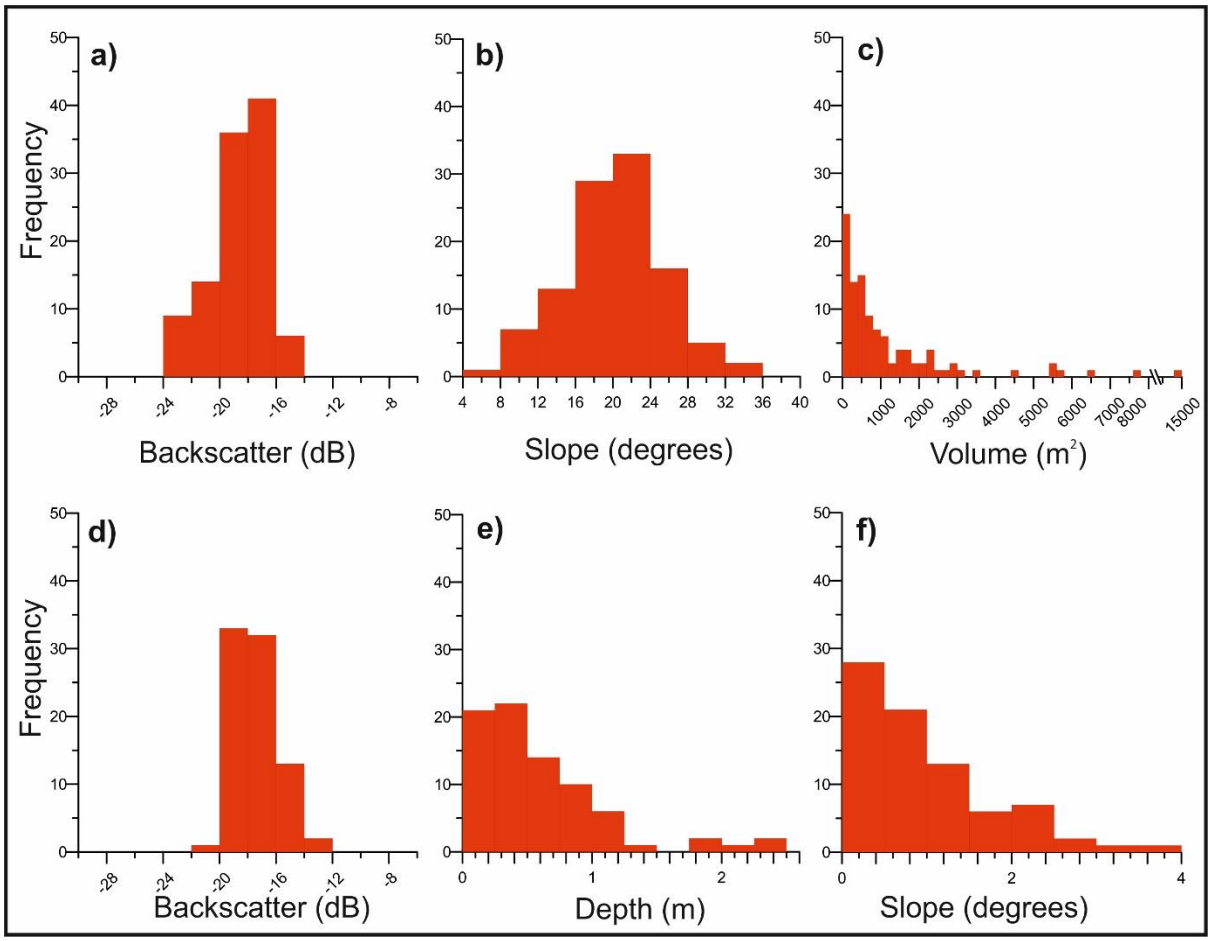

Figure 4 a) Backscatter histogram for the downslope Moira Mounds; b) slope histogram for the downslope Moira Mounds; c) mound volume histogram for the downslope Moira Mounds; d) backscatter histogram for the scour pits; e) depth histogram of the scour pits and; f) slope histogram for the scour pits.

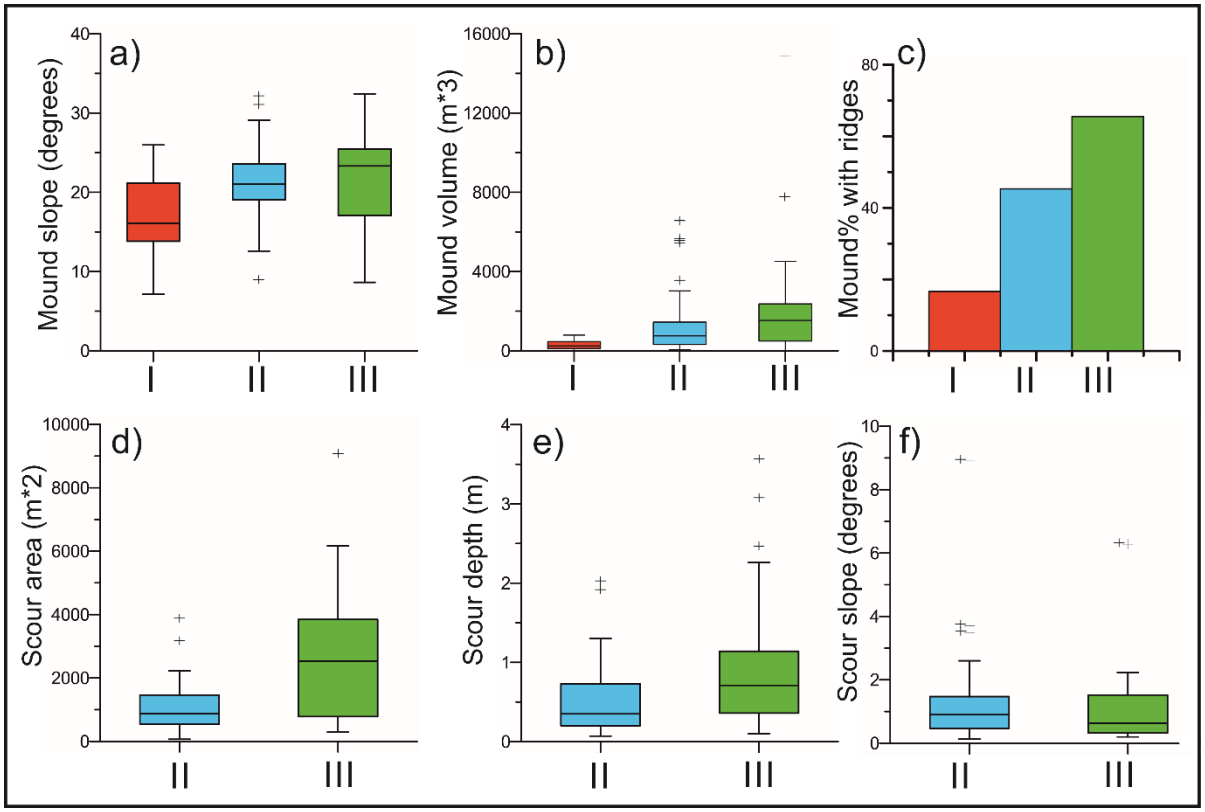

787

788 *Figure 5 Box & whiskers plots showing the distribution of the minimum, maximum, 1st quartile,*

789 *3rd quartile and mean values of Type I, II and III mounds for a) slope; b) volume; c) bar chart of*

790 *percentage that occur with ridge-like features; d) scour area; e) scour depth and; f) slope.*

791 *Outliers symbolised by "+" symbol.*

792

793

794

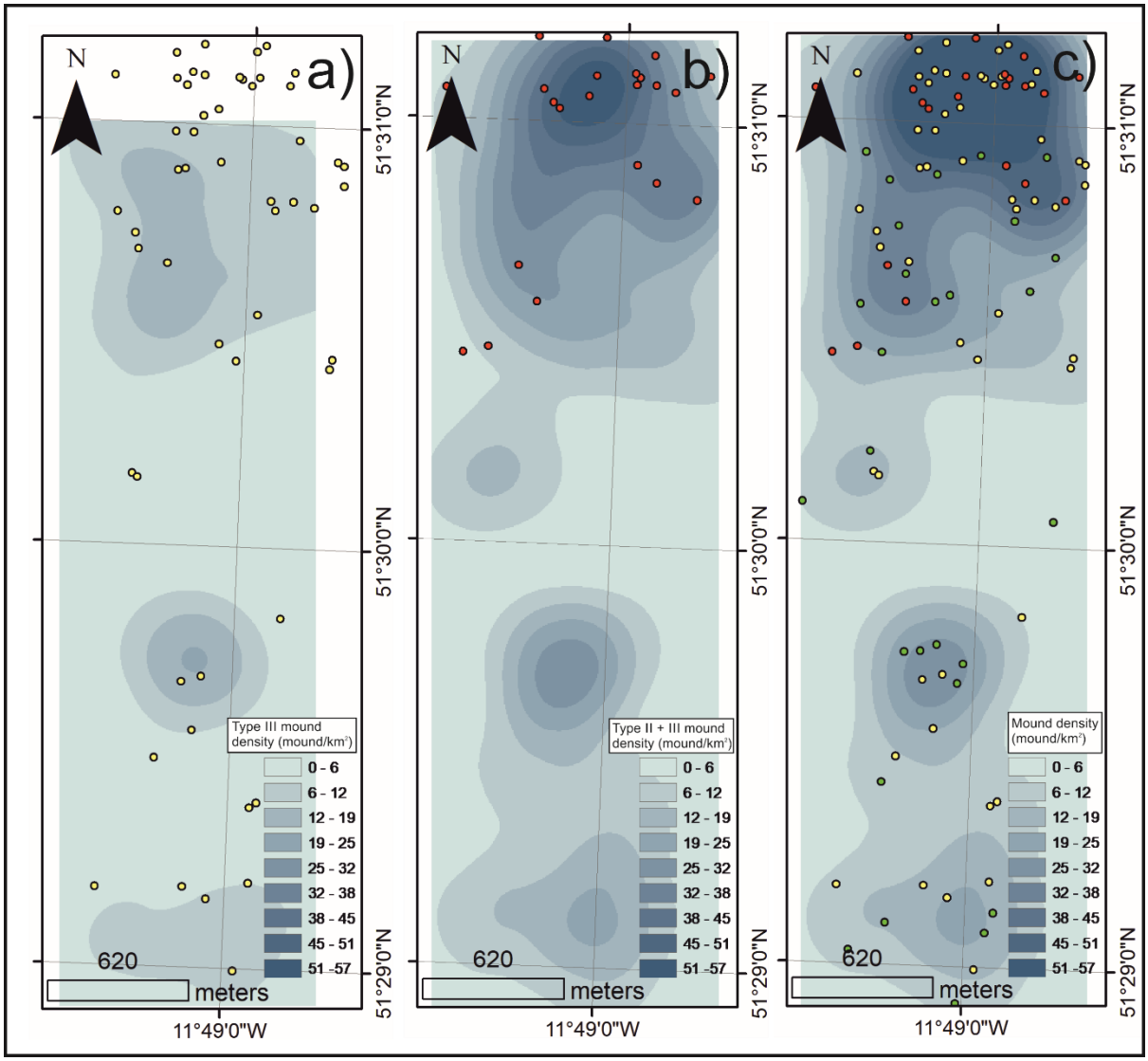

795

796 *Figure 6 Mound density maps a) Type III mound density raster with Type II mound points overlaid*

797 *(yellow); b) Type III and type II mound density raster with Type I mound points overlaid (red); c) all*

798 *mound density raster overlaid by the distribution of all mounds in the study area (yellow = Type II;*

799 *red = Type I and; green = Type III). Density is expressed as number of mounds per km^2 over a*

800 *neighbourhood of 460 m.*

801

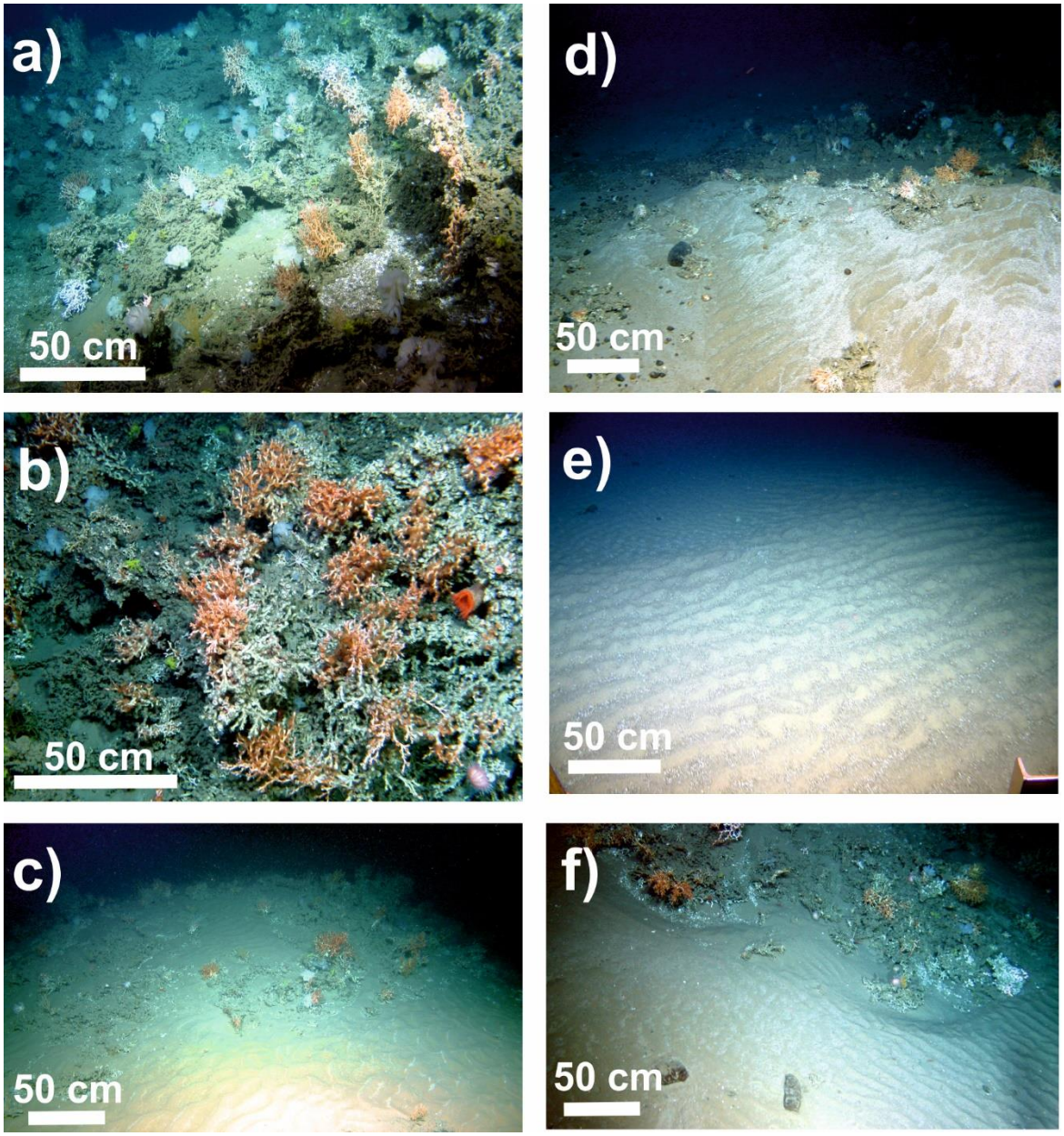

Figure 7 a) Surface of a Moira Mound; b) close up image of large and densely-packed coral colonies, mostly Lophelia pertusa; c) a small (Type I) Moira Mound showing sparse coral colonies; d) coral ridge within a scour pit; e) off-mound sinuously rippled sands; f) scouring around perimeter of mound.

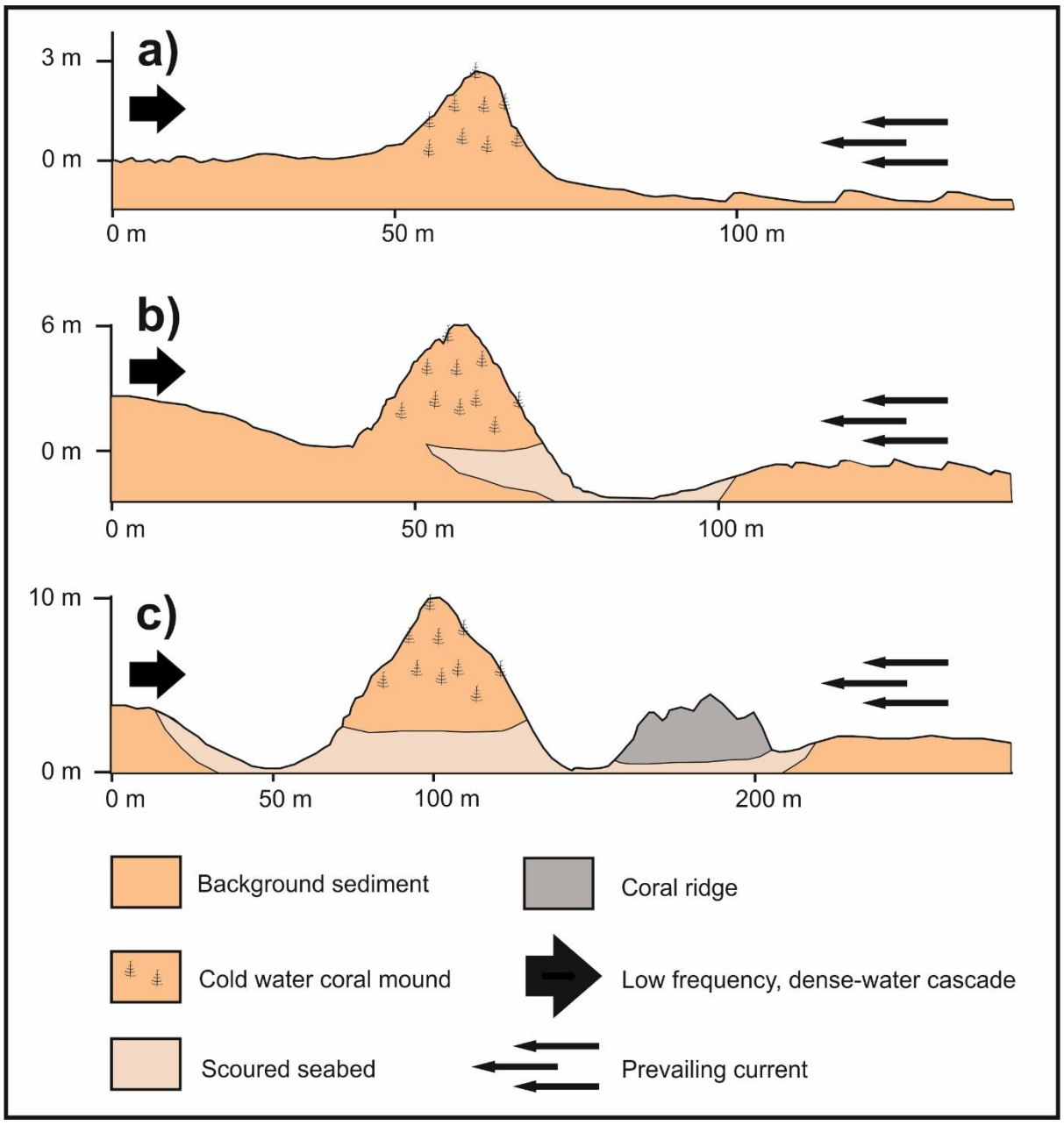

Figure 8a) Schematic of Type I mound local sedimentary environment where the mounds are 3 m in height, with a relatively gentle slope and no scouring; 8b) schematic of Type II mound local sedimentary environment where the mound has now developed to 6 m in height, poorly developed scour occurs at the base of the mounds and the slope has steepened; 8c) schematic of Type III mound local sedimentary environment where the mound has now developed to 10 m in height, the scour is well-developed, encircling the mound and coral ridges have developed within this scour pit.

816

Sample ID	**BC_23**	**BC_28**	**BC_21**	**BC_33**	**BC_31**	**BC_25**	**BC_26**
Mean grain size (µm)	267.8	441.3	215.4	111.8	209.5	225	176
Textural group	Muddy sand	Sand	Sand	Muddy sand	Sand	Sand	Sand
Erosional Velocity cm s^{-1} (Soulsby, 1997)	36	39	36	34	36	36	36

817

818 *Table 1 showing sediment sample grain size characteristics and erosional velocities after*

819 *Soulsby, 1997.*

820